# Study of the $\beta$-delayed neutron decay of $^{18}$N

K. W. Scheller, J. Görres, J. G. Ross, and M. Wiescher
*Department of Physics, University of Notre Dame, Notre Dame, Indiana 46556*

R. Harkewicz* and D. J. Morrissey
*National Superconducting Cyclotron Laboratory, and Department of Chemistry, Michigan State University, East Lansing, Michigan 48824*

B. M. Sherrill and M. Steiner
*National Superconducting Cyclotron Laboratory, and Department of Physics and Astronomy, Michigan State University, East Lansing,Michigan 48824*

N. A. Orr† and J. A. Winger‡
*National Superconducting Cyclotron Laboratory, Michigan State University, East Lansing, Michigan 48824*
(Received 27 August 1993)

The $\beta$-delayed neutron decay of $^{18}$N has been studied using a time-of-flight array with high efficiency. The $^{18}$N ions were produced by fragmentation of a $E/A = 75$ MeV $^{22}$Ne beam. Transitions to nine neutron unbound states have been observed with a total branching ratio of $2.2 \pm 0.4\%$. The results are compared with measurements of the decay to $\gamma$- and $\alpha$-emitting states and the differences between the present results and a recent measurement of the $P_n$ value are discussed.

PACS number(s): 23.90.+w, 23.60.+e, 21.10.Pc, 27.20.+n

## I. INTRODUCTION

The $\beta$-decay of $^{18}$N was first observed by Chase *et al.* [1] who measured the $\beta$-transition to the 4.46 MeV level ($J^\pi = 1^-$) in $^{18}$O and found a half-life of 630±30 ms. The resulting log$ft$ value of 4.8 restricted the ground-state spin of $^{18}$N to $(0\text{–}2)^-$. More recently, Olness *et al.* [2] measured the $\gamma$-decay following the $\beta$-decay of $^{18}$N using a Ge(Li) detector with high energy resolution and found six additional transitions to the $^{18}$O levels at 1.98 ($2^+$), 5.53 ($2^-$), 6.20 ($1^-$), 6.35 ($2^-$), 6.88 ($0^-$), and 7.77 ($2^-$) MeV. The observed half-life of 624±12 ms is in good agreement with the earlier value. The resulting relative branching ratios were converted to absolute $\beta$-decay branching ratios assuming a total branching ratio to non-$\gamma$-emitting states of 15±6% (3% to the ground state and 12% to $\alpha$- and neutron-emitting states) as suggested by shell model calculations [2]. The resulting log$ft$ value for the transition to the $0^-$ state at 6.88 MeV requires a ground-state spin of $1^-$ for $^{18}$N.

The $\beta$-delayed $\alpha$-decay of $^{18}$N has been studied by Zhao *et al.* [3]. They observed two narrow $\alpha$ groups which correspond to the $\beta$-decays to the known $1^-$ states at 7.62 and 8.04 MeV. In addition, a broad $\alpha$ group was seen at an excitation energy of 9.00 MeV with a width of about 500 keV. The total branching ratio to $\alpha$-emitting states is 12.2±0.6%. The nature of the broad $\alpha$ group is not clear. The experimental data can neither rule out a single broad group nor several unresolved groups. This broad peak can most likely contain only $J^\pi = 1^-$ states, because the $\beta$-decay of $^{18}$N ($J^\pi = 1^-$) populates in first-order only states with spin $0^-$, $1^-$, and $2^-$ and the $\alpha$-decay allows only states with natural parity. A single, broad peak is favored, however, over several unresolved groups for the following two reasons: (1) Six states are known [4] in the relevant energy region, but fitting the structure with these states [3] led to widths much larger than previously observed [4]; (2) While shell-model calculations [3] predict six $1^-$ states above the neutron threshold at $S_n = 8.044$ MeV, it seems unlikely that all should fall within 0.8 MeV when the calculations spread them over an energy range of 3 MeV. If this group indeed represents a single, broad state, then this state could be the $^{14}$C+$\alpha$ analog of the $^{12}$C+$\alpha$, $1^-$, state in $^{16}$O at 9.6 MeV, as suggested by Millener and Warburton [5] on the basis of systematics and semi-empirical arguments based on SU$^3$. This identification would require that the $\alpha$-width represents most of the total width of the state, and thus this state should be only weakly populated in the neutron channel.

A $P_n$ value of 14.3±2.0% for the $\beta$-delayed neutron decay of $^{18}$N has been measured by Reeder *et al.* [6]. Thus the combined branching ratio to particle emitting states is 26.5%, about twice the value assumed by Olness *et al.* [1]. Their branching ratios for the decay to $\gamma$-emitting states should therefore be normalized by a factor of 0.83.

---

*Present address: Argonne National Laboratory, Argonne, IL 60439.
†Present address: LPC-ISMRA, Boulevard du Marechal Juin, 14050 Caen Cedex, France.
‡Present address: Cyclotron Institute, Texas A&M University, College Station, TX 77843.

0556-2813/94/49(1)/46(5)/$06.00  

We have measured the $\beta$-delayed neutron decay of $^{18}N$ using a time-of-flight neutron detector array to complete the spectroscopy of the $\beta$-decay of $^{18}N$ and to search for a possible broad state in $^{18}O$ as indicated by the $\beta$-delayed $\alpha$-decay [3]. Our experimental setup will be described in Sec. II and the results will be presented in Sec. III followed by a discussion of these results in Sec. IV.

## II. EXPERIMENTAL SETUP

A $^{18}N$ beam was produced at the National Superconducting Cyclotron Laboratory at Michigan State by fragmentation of a 75 MeV/A $^{22}Ne$ beam impinging on a Beryllium target. The reaction fragments were separated by the A1200 separator using its momentum-loss achromat mode. A detailed description of the A1200 is given in Ref. [7]. The medium acceptance mode of the A1200 [7] was used for this experiment with a 300 mg/cm$^2$ thick Al degrader. The average purity of the $^{18}N$ beam was 85.9% with an intensity of 1400/s. The main impurity during the experiment was $^{20}O$ (13.7%). However, $\beta$-delayed neutron decay of $^{20}O$ is energetically not possible [4]. The only observed $\beta$-delayed neutron emitter was $^{16}C$ with an intensity of 0.4% of the beam.

The $^{18}N$ ions passed through a thin kapton window (0.25 mm thick) into air and were stopped in a thin plastic detector (BC412, 2 cm by 2.5 cm by 1 cm thick) which was positioned in the center of a neutron detector array (see Fig. 1 of Ref. [9]). Aluminum degraders and a Si detector were placed in front of this implantation detector. The thickness of the degraders was adjusted to stop the ions in the center of the implantation detector. The energy loss in the Si detector in combination with the time-of-flight, derived from the rf frequency of the cyclotron allowed an on-line particle identification. The implantation detector was surrounded by 15 large area neutron detectors (BC412, 157 cm by 7.6 cm by 2.54 cm thick) with a curvature radius of 1 m. The neutron detector array covered a solid angle of 14.3% of $4\pi$. The detector has been used previously to measure the $\beta$-delayed $n$-decay of $^{15}B$ [9] and a detailed description of the detector system can be found in Ref. [9].

The time signal of the implantation detector served as the start of a time-of-flight measurement to any of the neutron detectors. Time zero was deduced from the position of a prompt peak which was produced by relativistic electrons and the time spectra were calibrated using an electronic time calibrator. All individual time spectra were gain matched and added. The effective flight path (100.9$\pm$0.2 cm) was determined form the time-of-flight of neutrons from the $\beta$-delayed neutron decay of $^{16}C$ and $^{17}N$ which were measured using the same setup (Fig. 1). These decays produce neutrons with well-known energies [8] of $E_n$(lab)=0.808 and 1.715 MeV ($^{16}C$), and of 1.161 and 1.689 MeV ($^{17}N$). The time resolution is determined by the electronic resolution ($\approx$1 ns) and the uncertainty of the flight path ($\Delta l$ = 4.3 cm) due to the dimensions of start and stop detectors. The absolute detection efficiency as a function of the neutron energy was calculated from the observed intensities of the calibration lines and the well-known branching ratios of $^{16}C$ and $^{17}N$ [8]. The

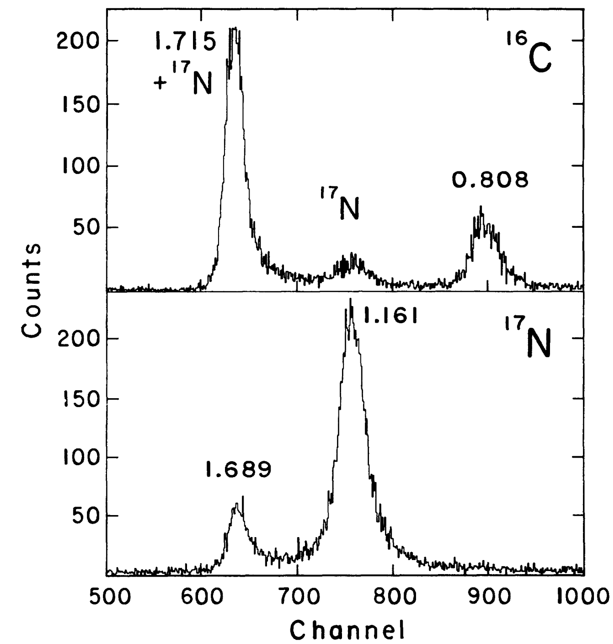


FIG. 1. Time-of-flight neutron spectra following the $\beta$-decay of $^{16}C$ (top) and $^{17}N$ (bottom). The neutron energies (in MeV) are given in the laboratory system. A small $^{17}N$ contamination can be seen in the $^{16}C$ spectrum.

efficiency curve (Fig. 2) was extended to 4.5 MeV using Monte Carlo calculations matched to the experimental values at 1.7 MeV. It has been shown [9] that these calculations agree with the measured relative efficiency within 10%. The efficiency increases sharply with energy at low energies and varies slowly with energy above 1.6 MeV resulting in an effective lower threshold of about 1 MeV. The total efficiency (including the solid angle) is $2.0 \pm 0.2\%$ at a neutron energy of 1.7 MeV.

The $^{18}N$ data ($t_{1/2}$ = 624 $\pm$ 12 ms) were measured in a beam on/beam off cycle, where the $^{18}N$ ions were

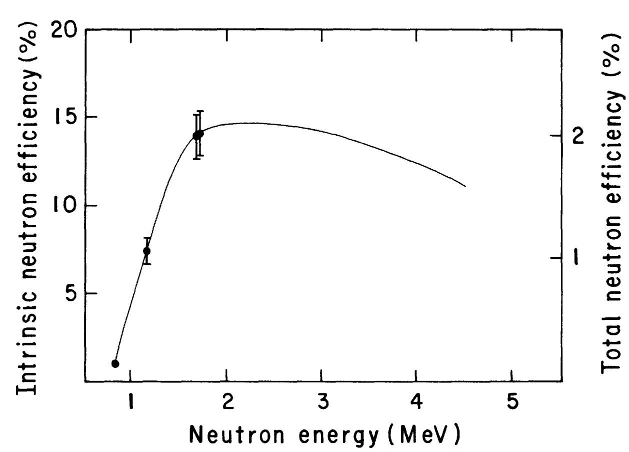


FIG. 2. Neutron efficiency as a function of the neutron energy; for details see text. The left-hand scale gives the intrinsic neutron efficiency of the detectors. The right-hand scale is the total neutron efficiency, where the solid angle has been included.

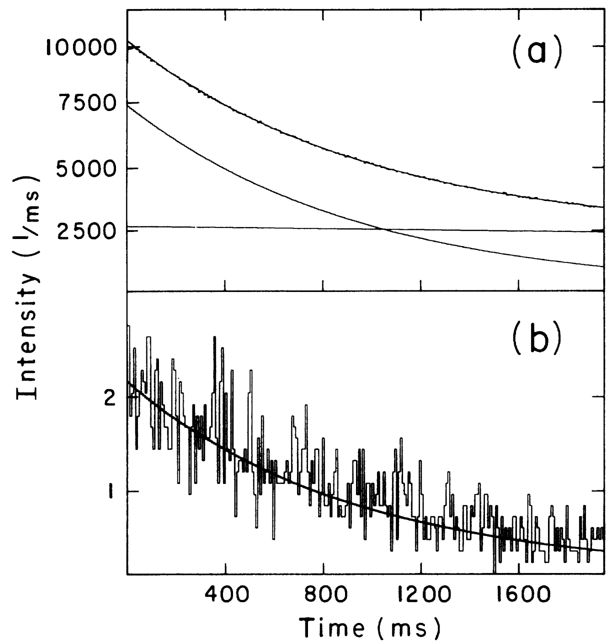


FIG. 3. Half-life spectra measured during one of the $^{18}$N runs. Shown are (a) the ungated half-life spectrum and (b) a half-life spectrum gated on the neutron group at 2.47 MeV.

implanted for 2.14 s and the decay was measured for 2.01 s. The cycle was controlled by an electronic clock and the primary beam was interrupted during the beam off period by applying a logical gate signal to a fast shifter in the rf transmitter of one of the dees of the cyclotron [10]. At the beginning of each beam off period a real time clock was started and the time of each event was recorded. A fit to the resulting half-life spectrum allowed the extraction of the total number of observed decays (Fig. 3).

## III. EXPERIMENTAL RESULTS

The $^{18}$N data were taken in three separate runs and a total of $2.32\times10^7$ decays were observed. Figure 3(a) shows one of the measured half-life spectra, which could be fitted with two exponential components. During the fit the well-known [4] half-lives of $^{18}$N (624±12 ms) and $^{20}$O (13.57±0.1 s) were held constant. The observed neutron spectrum is shown in Fig. 4. Eight neutron lines with energies of $E_n$(lab) = 1.16 ± 0.02, 1.35±0.02, 1.55±0.02, 1.77±0.02, 2.07±0.03, 2.46±0.03, 2.78±0.03, and 3.26±0.03 MeV were seen. An additional neutron line at 0.99 ±0.03 MeV cannot be excluded. The peaks were fitted assuming a Gaussian peak shape and the observed widths of all lines are within the errors in agreement with the expected experimental resolution increasing with neutron energy from 100 to 400 keV. To account for the $^{16}$C background, a neutron line at 1.715 MeV has been included in the fit. Position and shape of this line was determined from the $^{16}$C spectrum (Fig. 1). The main uncertainty of the fit is the exact shape of the background. In principle, one expects a background consisting of a constant contribution caused by random

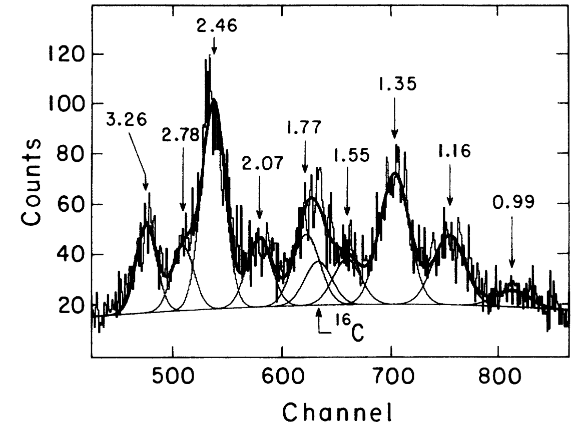


FIG. 4. Time-of-flight neutron spectrum of $^{18}$N. The data were fitted with a Gaussian line shape and a slightly curved background. A $^{16}$C line at 1.715 MeV has been included in the fit (see text for details).

coincidence events and a smoothly increasing background toward lower energies due to multiple scattering [9]. This last component depends on the composition of the neutron spectrum to be fitted. In the present case the high peak density did not allow a unique determination of the shape of the background. The fit shown represents a compromise between a flat background and a background with the maximum curvature allowed by a fit to the data. This uncertainty does not change the energies within the quoted errors. The influence of the background on the neutron intensity has been estimated to be 15%. The total branching ratio of $^{18}$N to neutron unbound levels is 2.2±0.4%. These results are summarized in Table I. Half-life spectra gated on the individual neutron lines were also created. The observed half-life for each line is within the errors in good agreement with the known half-life of $^{18}$N. Figure 3(b) shows the half-life spectrum gated on the neutron line at $E_n$(lab) = 2.46 MeV. The spectrum can be fitted with a single exponential and the resulting half-life of 630±20 ms is in excellent agreement with the literature value [4].

The log$ft$ values for the observed transitions were calculated from the known half-life of $^{18}$N and the observed branching ratios and are listed in Table I. The values are typical for allowed transitions and limit the spins of the observed levels to $J^\pi = (0–2)^-$.

## IV. DISCUSSION

The $^{18}$O excitation energies from the present experiment are compared in Table II with the compilation of $^{18}$O levels by Ref. [4]. Six of the observed states correspond to known states in $^{18}$O while the remaining three states at 9.27, 10.24, and 11.49 MeV correspond to previously unobserved states. None of the known states with spin assignments other than $(0–2)^-$ have been observed in the present experiment in agreement with the spin selection rules.

No evidence was found (see Fig. 4) for the strong pop-

TABLE I. Summary of the experimental results for the $\beta$-delayed neutron decay of $^{18}$N (all energies are in MeV).

| $E_n$(lab) | $E_x(^{18}\text{O})$ | BR (%) | log$ft$ | $J^\pi$ |
|---|---|---|---|---|
| (0.99±0.03) | (9.09±0.03) | 0.16±0.03 | 6.27±0.09 | $(0\text{–}2)^-$ |
| 1.16 ±0.02 | 9.27 ±0.02 | 0.39±0.09 | 5.81±0.12 | $(0\text{–}2)^-$ |
| 1.35 ±0.02 | 9.47 ±0.02 | 0.47±0.09 | 5.64±0.09 | $(0\text{–}2)^-$ |
| 1.55 ±0.02 | 9.69 ±0.02 | 0.14±0.03 | 6.07±0.10 | $(0\text{–}2)^-$ |
| 1.77 ±0.02 | 9.91 ±0.02 | 0.17±0.03 | 5.88±0.08 | $(0\text{–}2)^-$ |
| 2.07 ±0.02 | 10.24±0.03 | 0.16±0.03 | 5.75±0.09 | $(0\text{–}2)^-$ |
| 2.46 ±0.03 | 10.65±0.03 | 0.43±0.09 | 5.08±0.10 | $(0\text{–}2)^-$ |
| 2.78 ±0.03 | 10.99±0.03 | 0.13±0.03 | 5.39±0.10 | $(0\text{–}2)^-$ |
| 3.26 ±0.03 | 11.49±0.03 | 0.19±0.04 | 4.85±0.10 | $(0\text{–}2)^-$ |
| Total[a] | | 2.2±0.4 | | |

[a]The common errors of the total efficiency (10%) and the uncertainty of the shape of the background (15%) have been added after the summing.

ulation of a broad state at $E_x \sim 9$ MeV. No fit was attempted to obtain an upper limit for a transition to such a state because of the unknown shape of the background in the region of interest. However, an upper limit for the branching ratio of $\leq 1\%$ was deduced from the total number of counts in the relevant energy range. These data were corrected for the lower energy threshold of the detector at an excitation energy of $\approx 9$ MeV. Comparing this number with the branching of 3.6% observed in the $\alpha$ channel [3], it can be concluded that most of the observed width corresponds to the $\alpha$ width of this state, if the broad structure is in fact a broad state. This result would make it likely that this state is a $^{14}$C+$\alpha$ cluster state analog of the $^{12}$C+$\alpha$ $1^-$ state in $^{16}$O at 9.6 MeV [5]. Alternatively, Zhao *et al.* [3] also investigated the possibility of six broad, unresolved states and presented the results of a corresponding fit to the broad structure observed in the $\beta$-delayed $\alpha$-decay of $^{18}$N. Three of the six states are above the energy threshold of this experiment (see Table II), but only one state lines up with a state observed in the neutron channel. The branching ratio to this state at 9.09 MeV of 0.16% is small compared to the value of the $\alpha$ channel of 0.97%. Therefore at least three of the six states contain appreciable $\alpha$ strength, $\Gamma_\alpha > \Gamma_n$ in this alternative scenario. Additional experiments, e.g., a high-resolution study of the $\beta$-delayed $\alpha$-decay, are necessary to resolve the uncertainty of the exact nature of this structure.

TABLE II. Comparison of the present $^{18}$O excitation energies with the literature [3,4] (all energies in MeV ± keV).

| Present | Ref. [4] | $J^\pi$ | Ref. [3][a] |
|---|---|---|---|
| | 9.03 | nat. $\pi$ | |
| (9.09±30) | (9.10) | nat. $\pi$ | 9.07±20 |
| | | | 9.21±20 |
| 9.27±20 | | | |
| | 9.361±6 | $(3^-)$ | 9.36±20 |
| | 9.418±18 | | |
| 9.47±20 | 9.48±24 | | |
| 9.69±20 | 9.672±7 | | |
| | 9.713±7 | | |
| 9.91±20 | 9.890±11 | | |
| | 10.118±10 | $3^-$ | |
| 10.24±30 | | | |
| | 10.295±20 | $4^+$ | |
| | 10.396±9 | $3^-$ | |
| 10.65±30 | 10.595±15 | | |
| | 10.82±20 | | |
| | 10.91±20 | | |
| 10.99±30 | 10.99±20 | | |
| | 11.13±20 | | |
| | 11.39±20 | $(2^+)$ | |
| | 11.41±20 | $(4^+)$ | |
| 11.49±30 | | | |
| | 11.62±20 | $5^-$ | |

[a]See text.

A total branching ratio of 2.2±0.4% to neutron unbound states has been observed in this experiment compared to a measured $P_n$ value of 14.3±2.0% [6]. The unobserved branching of $\approx 12\%$ must proceed to one or several states within the narrow excitation range between $E_x = 8.04$ MeV (neutron-threshold) and $E_x = 9.0$ MeV (the lower energy threshold of this experiment). To populate a state in this excitation range with a branching ratio of 12% would require a log$ft$ value of 4.0 to 4.5. This assumption is supported by shell-model calculations [3,6]. While these calculations do not predict that $0^-$ and $1^-$ states are populated with sufficient strength, a $2^-$ state is predicted [6] above the neutron threshold with log$ft \approx 4.1$. Possible candidates for such a state are the levels at $E_x = 8.521$ and 8.660 MeV. Both states are the only known levels in the relevant excitation range which have not been observed in $\alpha$-induced reactions on $^{14}$C as expected for a state with unnatural parity. These states were only seen in the $^{19}$F$(t,\alpha)^{18}$O [11,12] and the $^{16}$O$(t,p)^{18}$O [13] reactions. Their weak population in the $^{16}$O$(t,p)$ reaction [13] suggests an unnatural parity for these states.

We would like to thank the entire staff of the NSCL, especially R. Fox, for their assistance during this experiment. This work is supported by the National Science Foundation under Grant Nos. PHY91-00708 (Notre Dame) and PHYS89-13815 (MSU).

[1] L. F. Chase Jr., H. A. Grench, R. E. McDonald, and F. J. Vaughn, Phys. Rev. Lett. **13**, 665 (1964).
[2] J. W. Olness, E. K. Warburton, D. E. Alburger, C. J. Lister, and D. J. Millener, Nucl. Phys. **A373**, 13 (1982).
[3] Z. Zhao, M. Gai, B. J. Lund, S. L. Rugari, D. Mikolas, B. A. Brown, J. A. Nolen, and M. Samuel, Phys. Rev. C **39**, 1985 (1989).
[4] F. Ajzenberg-Selove, Nucl. Phys. **A475**, 1 (1987).
[5] E. K. Warburton and J. Millener (private communication, 1990).
[6] P. L. Reeder, R. A. Warner, W. K. Hensley, D. J. Vieira, and J. M. Wouters, Phys. Rev. C **44**, 1435 (1991).
[7] B. M. Sherrill, D. J. Morrissey, J. A. Nolan, and J. A. Winger, Nucl. Instrum. Methods **B56/57**, 1106 (1991).
[8] F. Ajzenberg-Selove, Nucl. Phys. **A460**, 1 (1986).
[9] R. Harkewicz, D. J. Morrissey, B. A. Brown, J. A. Nolan, N. A. Orr, B. M. Sherrill, J. S. Winfield, and J. A. Winger, Phys. Rev. C **44**, 2365 (1991); R. Harkewicz, Ph.D. thesis, Department of Chemistry, Michigan State University, 1992.
[10] D. Mikolas, B. A. Brown, W. Benenson, L. H. Harwood, E. Kashy, J. A. Nolan, B. M. Sherrill, J. Stevenson, J. S. Winfield, Z. Q. Xie, and R. Sherr, Phys. Rev. C **37**, 766 (1988).
[11] S. Hinds, H. Marchant, and R. Middleton, Nucl. Phys. **38**, 81 (1962).
[12] J. W. Olness, E. K. Warburton, and J. A. Becker, Phys. Rev. C **7**, 2239 (1973).
[13] M. E. Cobern, L. C. Bland, H. T. Fortune, G. E. Moore, S. Mordechai, and R. Middleton, Phys. Rev. C **23**, 2387 (1981).